

**OPEN ACCESS**

## Evaluation of the sensitivity and response of IR thermography from a transparent heater under liquid jet impingement

To cite this article: H D Haustein *et al* 2012 *J. Phys.: Conf. Ser.* **395** 012083

View the [article online](#) for updates and enhancements.

### Related content

- [Experimental Study of Endwall Heat Transfer in a Linear Cascade](#)  
Lei Wang, Bengt Sundén, Valery Chernoray *et al.*
- [Experimental study of flow boiling heat transfer in a rectangular minichannel by using various enhanced heating surface](#)  
Magdalena Piasecka
- [Effect of Thermal Boundary Condition on Heat Dissipation due to Swirling Jet Impingement on a Heated Plate](#)  
Karl J Brown, Gerry Byrne, Tadhg S O'Donovan *et al.*



The banner features a decorative top border with a repeating pattern of red, white, and blue diagonal stripes. On the left, the ECS logo is displayed in blue and green, followed by the text 'The Electrochemical Society' and 'Advancing solid state & electrochemical science & technology'. In the center, the text '239th ECS Meeting with IMCS18' is prominently displayed in a large, bold, dark blue font. Below this, 'DIGITAL MEETING • May 30-June 3, 2021' and 'Live events daily • Free to register' are written in a smaller, dark blue font. On the right side, there is a stylized graphic of a person's head with glowing blue lines and icons representing technology and connectivity. A red button with the text 'Register now!' is positioned at the bottom right of the banner. A small logo with the number '18th' is also visible in the upper right area of the banner.

# Evaluation of the sensitivity and response of IR thermography from a transparent heater under liquid jet impingement

H D Haustein<sup>1</sup>, W Rohlf, F Al-Sibai and R Kneer

Institute of Heat and Mass Transfer (WSA), RWTH Aachen University, Aachen  
52056, Germany

Email: haustein@wsa.rwth-aachen.de

**Abstract.** The feasibility of a visible/IR transparent heater and its suitability for IR thermography is experimentally examined. The most common transparent conductive coating, Indium Tin Oxide (ITO), is quite reflective and its optical properties depend on thickness and manufacturing process. Therefore, the optical properties of several thicknesses and types of ITO, coated on an IR window (BaF<sub>2</sub>), are examined. A highly transparent Cadmium Oxide (CdO) coating on a ZnS window, also examined, is found to be unusable. Transmissivity is found to increase with a decrease in coating thickness, and total emittance is relatively low. A thick ITO coating was examined for IR thermography in the challenging test case of submerged water jet impingement, where temperature differences were characteristically small and distributed. The measurements under steady state conditions were found to agree well with the literature, and the method was validated. Comparison of two IR cameras did not show the LWIR low-temperature advantage, up to the maximal acquisition rate examined, 1.3KHz. Rather the MWIR camera had a stronger signal to noise ratio, due to the higher emissivity of the heater in this range. The transient response of the transparent heater showed no time-delay, though the substrate dampens the thermal response significantly. Therefore, only qualitative transient measurements are shown for the case of pulsating free-surface jet impingement, showing that the motion of the hydraulic jump coincides with thermal measurements. From these results, recommendations are made for coating/window combination in IR thermography.

## 1. Introduction

The focus of the present study is the feasibility of IR thermography from a transparent heater, under steady and transient conditions. The method of temperature measurement by IR thermography is well established, relatively accurate and has a high spatial and temporal resolution [1]. Previous use of IR thermography for *transient* measurements has usually been based on micrometrically thin metal foils. These foils have the required mechanical strength together with a fast thermal response [2], i.e. negligible time delay and amplitude dampening. However, they do not provide optical access through the heater, which allows additional optical measurements to be performed simultaneously (such as PIV, LDV, Liquid Crystal thermography, Laser induced Fluorescence etc.).

For this reason transparent heaters, based on transparent conductive oxide coatings (TCOs), have been increasingly employed in research, ever since their introduction in the late 60's. Within the last decade, a clear leader in TCO performance (high transparency and high electrical conductance) has emerged – Indium Tin Oxide (ITO) [3]. However, the scarcity of Indium has raised concerns regarding its future widespread use.

To date, very few studies have attempted to combine IR thermography with transparent heaters. Bang et al. [4] showed qualitative measurements from an ITO coating, for the case of nucleate boiling.

---

<sup>1</sup> To whom any correspondence should be addressed.

Recently, Soriano et al. [5] have performed IR thermography from a transparent heater under spray impingement cooling, though no thermal images were presented, possibly due to relatively large uncertainties in the optical properties and measurements (see Soriano [6]). The finding of these properties and reduction of uncertainties is addressed in the following section.

In order to evaluate the performance of IR thermography from a transparent heater the test case of submerged impinging jet cooling was chosen. This test case is relatively easy to set up experimentally, though presents significant challenges to temperature measurement methods: wall temperature varies strongly in space (and if desired in time too) and due to high heat transfer temperature differences are characteristically small (typically less than 1°C in the stagnation zone). Additionally, this test case has been widely studied in liquids [7,8] and the many experimental correlations allow easy comparison and validation of measured results.

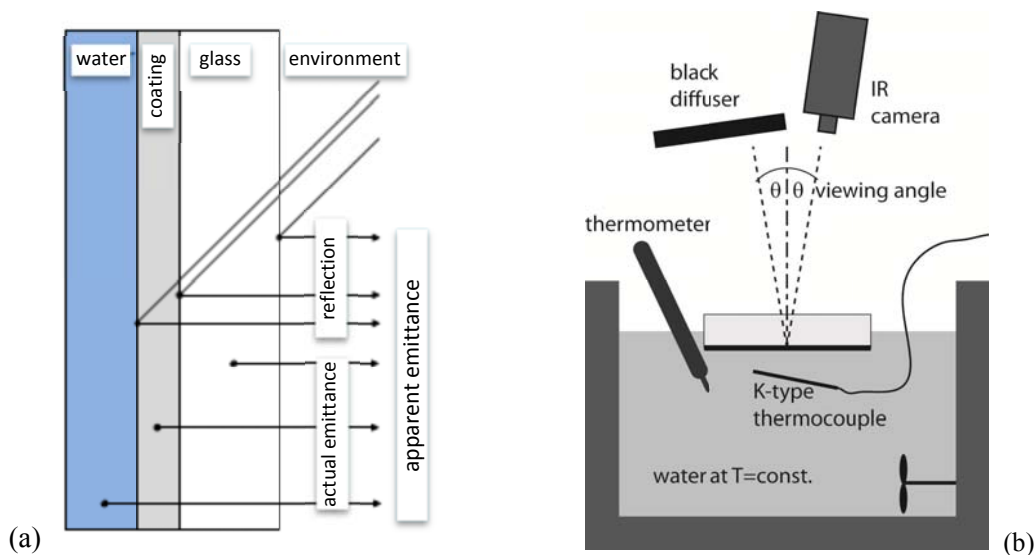


**Figure 1.** IR thermography from a layered, semi-transparent object: a) optical schematic of emittance; b) experimental system used for finding the emissivity of the coating.

In the present study IR thermography from a transparent heater is first addressed in a general way, wherein the crucial optical parameters are identified. This is followed by a closer examination of these optical parameters and their dependencies for several specific transparent heaters, with the goal of improving the current thermography performance. Once completed, a specific heater is chosen for the second half of the study that comprises an evaluation of the improved IR thermography method in a test-case experiment. In the test-case, impinging jets are examined at relatively low heat fluxes, with driving temperature differences of just a few degrees, where the required accuracy of 0.1°C is met. In this evaluation, two different cameras are compared, as well as steady and transient flow conditions.

## 2. An improved IR thermography method

Generally, the most important parameter in a complex heat exchange system is the value/distribution of the heat transfer coefficient. This value cannot be calculated for anything but the simplest configurations, and may vary strongly in time and space, as it is dependent on the flow field around the given geometry. The heat transfer coefficient is generally defined according to (1). It is convenient to perform experiments using a *thin film heater*, where  $q''$  can be assumed to be uniform, and under steady state conditions also constant. For the present study, a transparent conductive oxide was coated (submicron layer) onto a dielectric ceramic (glass) substrate, from which the wall temperature,  $T_w(x, y,$

$t$ ), is measured with high resolution in time and space, by employing IR thermography as described below, while  $T_{inf}$  is held constant at the jet outlet (here  $T_{inf}=40^{\circ}\text{C}\pm 0.1$ ).

$$h(x, y, t) = \frac{q''(x, y, t)}{T_w(x, y, t) - T_{inf}(x, y, t)} \quad (1)$$

### 2.1. IR thermography from a semi-transparent surface

Recently, Soriano et al. [5,6] have presented measurements taken from a ZnSe substrate coated with ITO, though high uncertainties were present (see Chap. 3, section E). The method described there, which is based on the ASTM 1933E guidelines, is followed here, though with several significant changes: i) due to the high reflectivity of ITO in the IR range, the emissivity is first found *in situ*, by employing a specific experimental system (see Fig. 1b); ii) all optical properties required for accurate *quantitative* measurements are retrieved; iii) and finally, time-averaging and image subtraction methods are employed to increase the sensitivity and reduce errors, wherever possible. This improved method allows not only quantitative measurement, but high sensitivity and accuracy also, as will be demonstrated in the second part of this study.

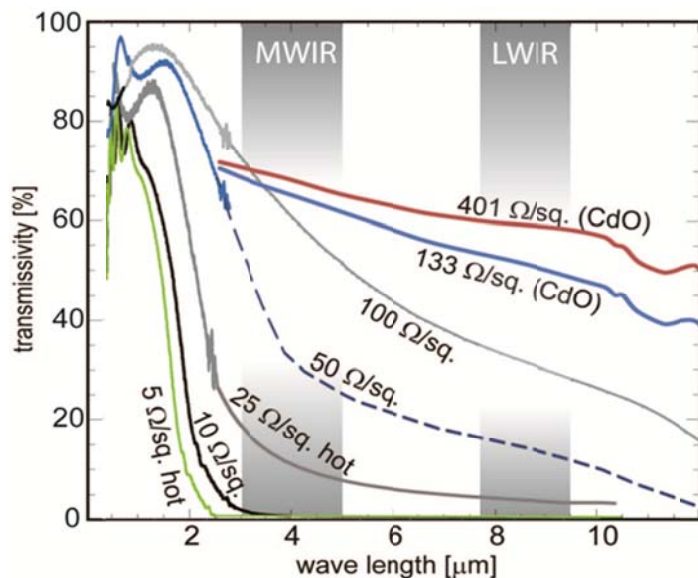


**Figure 2.** Transmissivity spectrum for various coatings of resistivity; ITO is Indium Tin Oxide (on BaF<sub>2</sub>) and CdO is Cadmium Oxide (on ZnS), “hot“ refers to annealing (350°C, for 4 hours); measurements courtesy of Diamond Coatings Ltd., UK, Centre for Solar Energy Research, Glyndŵr University, UK, and the Institute of organic chemistry, RWTH Aachen, Germany; the “Ω/sq.” symbol indicates Ohms per square section of coating; dashed line indicates interpolated value.

The main limitation to the use of IR thermography with transparent heaters is that the apparent (observed) emittance needs to be correctly converted to the actual temperature of the heater wall. The apparent emittance of a multi-layered, semi-transparent wall is depicted in Fig. 1a and given in Eq. (2).

$$W_a = (\rho_g + \tau_g \rho_c \tau_g + \tau_g \tau_c \rho_w \tau_c \tau_g) W_e + \varepsilon_g W_g + \varepsilon_c \tau_g W_c + \varepsilon_w \tau_c \tau_g W_w \quad (2)$$

In this equation,  $W$  represents the emitted radiance and the subscripts  $a$ ,  $w$ ,  $c$ ,  $g$ ,  $e$ , stand for *apparent*, *water*, *coating*, *glass* and *environment*, accordingly. Additionally, the Greek symbols  $\tau$ ,  $\varepsilon$ , and  $\rho$ , represent the optical properties of transmissivity, emissivity and reflectivity. The first term on the RHS (in brackets) is the reflection term and the following ones are the actual thermal emittance

terms. While the optical properties of the water and glasses used, BaF<sub>2</sub> (Barium Fluoride) or ZnS (Zinc Sulfide), are well-known and easily obtainable from the literature or the manufacturer, the optical properties of the coating vary strongly with the type of material and are highly dependent on thickness, manufacturing process and coating uniformity. For this reason, the total transmissivity (glass + coating) was directly measured and the emissivity of the coating was established through a specifically designed experimental system (see figure 1b) as will be described in the following. For identification of the most suitable type of coating, the optical properties were measured for several types of ITO and CdO (Cadmium Oxide) coatings. The ITO coatings were all applied to a highly transparent BaF<sub>2</sub> IR window, while the CdO was found to adhere better to a ZnS substrate.

Figure 2 shows the transmissivity measurements, performed in-house using the A-FTIR measurement method. These measurements revealed the well-known trend, whereby the transmissivity increases with a decrease in coating thickness. Similarly, additional coating thickness measurements revealed that the relative uniformity of the coatings (and therefore the uniformity of the imposed heat flux,  $q''$ ) scales with the coating thickness (inversely with the resistivity). The ITO was coated using the Magnetron sputtering technique that provided high uniformity (better than  $\pm 5\%$  for all samples), whereas the CdO coating was only available at experimental grade - MOCVD coating with uniformity varying radially from the center (up to 17% at 133 Ohm/sq. and up to 33% at 401 Ohm/sq.). The “hot” ITO coatings were also thermally annealed (at 350°C) for several hours, leading to a lower resistivity, better uniformity, and significantly *lower transmissivity* (compare coatings of similar thickness - 25 Ohm/sq. hot to 50 Ohm/sq., in figure 2).

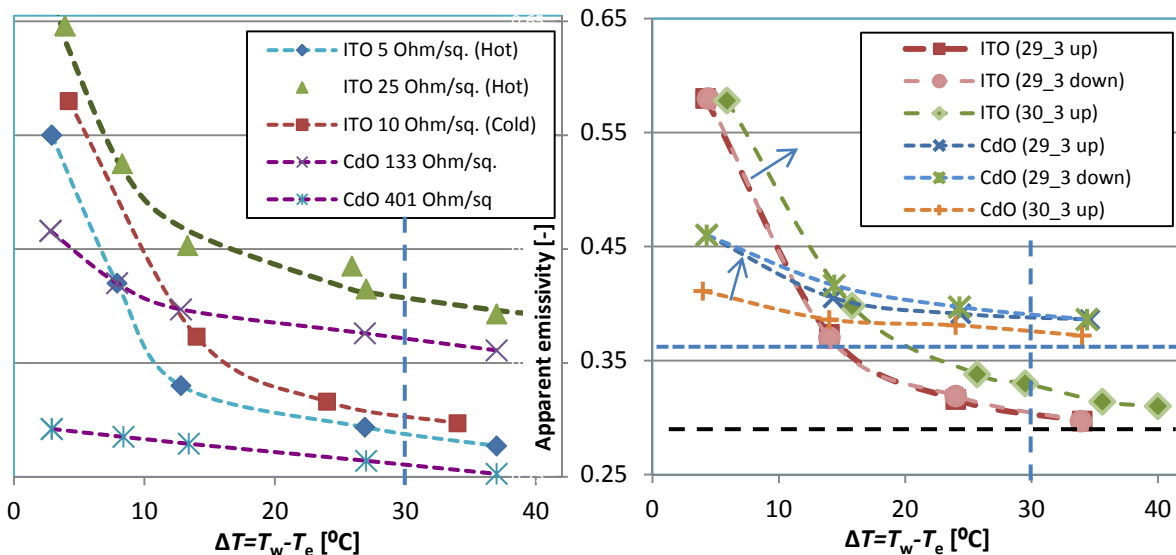


**Figure 3.** Emissivity of several transparent conductive coatings (LWIR), as dependent on: a) coating type and temperature elevation; b) Environment temperature (arrows indicate increase of  $\sim 1.3^\circ\text{C}$ ); Horizontal lines indicate end (converged) value, vertical lines - recommended minimum  $\Delta T$

In order to establish the coating emissivity from Eq. (2) a simpler form is first developed. In addition to the thin-film assumption normally used ( $T_c$  and  $T_w$  are equal), it is seen that the temperature of the glass is very close to that of the water, as the gas-side natural convection heat loss is three-orders of magnitude smaller than that on the regulated water-bath side. Furthermore, the emittances in Eq. 2 can be converted to black body equivalent temperatures within the IR camera software. Based on

pre-calibration in front of a highly accurate black-body, the conversion can be described by a parabolic curve,  $W_i=AT_i^2+BT_i+C$ . Combining these approximations lead to a simplified form of Eq. 2, as:

$$T_a \approx \sqrt{\frac{B^2}{4A^2} + (\rho_g + \rho_c \tau_g^2 + \rho_w \tau_g^2 \tau_c^2)(AT_e^2 + BT_e + C) + (\varepsilon_g + \varepsilon_c \tau_g + \varepsilon_w \tau_g \tau_c)(AT_w^2 + BT_w + C) - C} - \frac{B}{2A} \quad (3)$$

In this equation the calibration constants ( $A$ ,  $B$  and  $C$ ) are used for calculating the emissivity of the coating ( $\varepsilon_c$ ), based on the preset bath temperature ( $T_w$ ), measured environment temperature ( $T_e$ ), measured apparent temperature ( $T_a$ ) and the other optical properties. Alternately, if the calibration coefficients are not available, tolerable accuracy (around 8%) can be obtained by assuming that emissivity is proportional to temperature,  $W \sim T$ , within a limited range of temperatures (23-63°C), when  $T_w$  is at least 30°C above ambient, as recommended in ASTM 1933E.

Measurements were performed in the emissivity establishment setup (Fig. 1b) with a special focus on the Medium and Long Wave InfraRed ranges (MWIR - 3.5-5 $\mu$ m and LWIR - 7.7-9.4 $\mu$ m wavelength, accordingly), normally used in IR thermography. These measurements were introduced into Eq. 3 and the emissivity was calculated for the different coatings as shown in Fig. 3. In these experiments the wall temperature was imposed in the designated system. Emissivity *apparently* varied with wall temperature elevation (above environment), environment temperature and viewing angle. However, as the emissivity is a fixed, optical property is understood that the measured values asymptotically approach their actual value with increased temperature elevation.

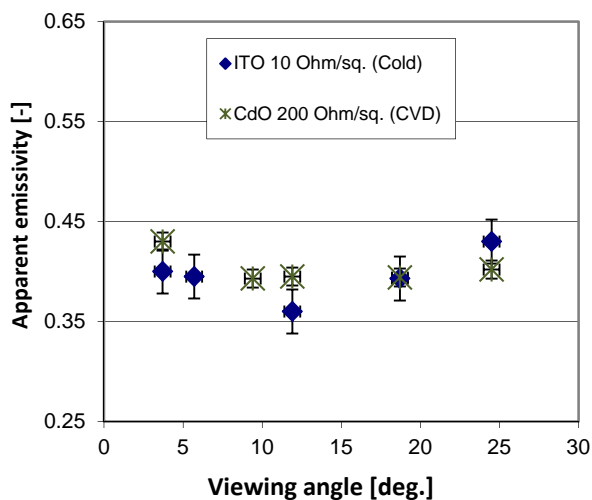


**Figure 4.** Viewing angle dependency of the emissivity in the LWIR range.

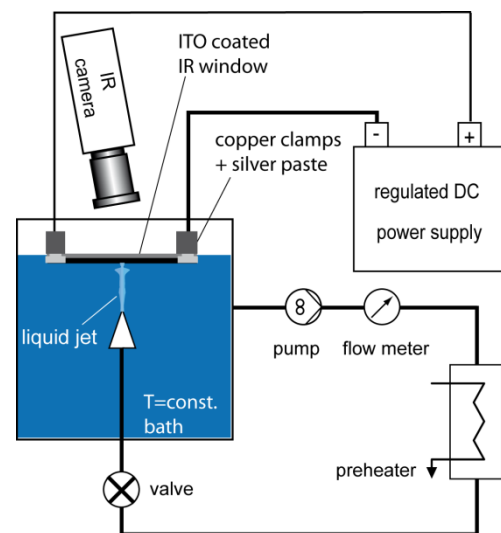


**Figure 5.** Schematic of experimental submerged jet-impingement system for validation.

Though the thinner transparent coatings have higher emissivity (and transmissivity), they have lower thickness uniformity leading to a higher uncertainty in thermal measurements. For this reason, only the emissivity of the thickest CdO and ITO coatings was examined more closely (CdO 133 Ohm/sq. and ITO 10 Ohm/sq. cold). Figure 3b shows repeated experiments under various conditions (increasing bath temperature/different environment temperature). Though values are sensitive to environment temperature, there is similar convergence to a similar end value, along an exponential

decay curve. The figure also demonstrates that the standard recommended temperature-elevation of 30°C (according to ASTM 1933E) is sufficient, and when unobtainable (temperature sensitive liquids, proximity to saturation or system limitation) an exponential convergence-curve can be used for better prediction. From additional measurements (not shown) it was found that the emissivity of the ITO coating in the MWIR range is about 30% higher than in the LWIR range, in accordance with the Fresnel equations for decreasing  $n$  and increasing  $k$  materials [9]. Viewing angle dependency of the emissivity value is shown in Fig. 4, where variation as high as 15% is found below 25 degrees. Therefore, it is recommended that measurements be conducted at viewing angles between 7 and 15 degrees - as done in the present study, (to avoid the “narcissus effect” and allow simultaneous access for high-speed photograph).

In subsequent experiments the CdO coating deteriorated rapidly, due to sensitivity to mild acids. Therefore no test-case experiments were performed with it and only the more robust 10 Ohm/sq. (cold) ITO coating was used, which is effectively opaque in the MWIR and LWIR range (see Fig. 2). Although the peak emittance in the given temperature range (40-60°C) occurs within the LWIR range (see [1]), the ITO has a higher emissivity in the MWIR range. It was found that the uncertainty of the measurement is not related to the strength of the overall signal (the IR sensor saturated below the maximal integration time, with both cameras), but rather due to the low Signal to Noise Ratio (SNR). The SNR is strongly influenced by the noise level of the sensor, and mostly by the reflection (inverse of the emissivity) of the coating. Therefore, the MWIR actually performed slightly better than the LWIR camera (up to an acquisition rate of 1.3Khz), though this trend is expected to reverse once higher acquisition rates (shorter integration time) are used.

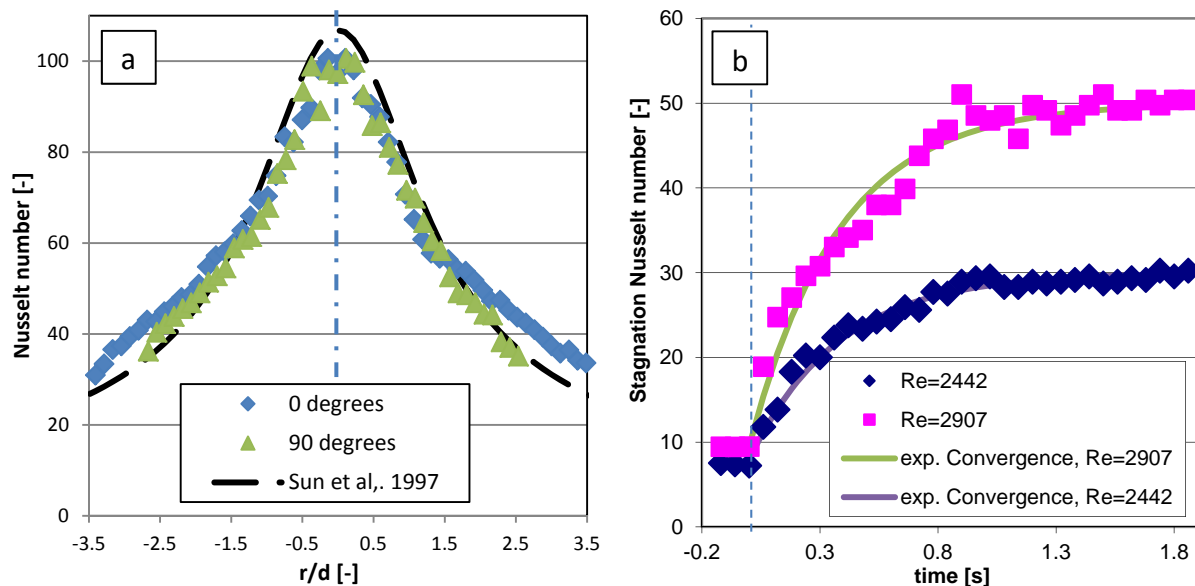


**Figure 6.** Submerged jet impingement: a) heat transfer distribution along two perpendicular lines crossing at the stagnation point, steady state conditions (MWIR camera,  $Re=3550$ ,  $q''=3.2W/cm^2$ ,  $z/d=5.3$ ); b) Stagnation Nusselt number for jet start-up (LWIR camera at 50fps and  $q''=3.2W/cm^2$ ).

### 3. Method evaluation through submerged jet impingement

For examination of the reliability of measurements and applicability of the chosen transparent heater (10Ohm/sq. ITO on a BaF<sub>2</sub> window) the well-known test case of submerged impinging jet cooling was

examined (see system setup in Fig. 5). The system is only briefly described, a more detailed description can be found in Haustein et al. [10]. In short, a temperature and flow regulated loop delivers deionized water through a valve to a 2mm (i.d.) nozzle. The jet exists the nozzle, passes through a bath of water held at the same temperature, and impinges upon the transparent heater located several diameters away. A uniform heat flux is imposed on the heater by regulated DC power supply and the wall temperature is measured by IR thermography (FLIR SC7500 in the MWIR and/or Cedip Jade 3 in the LWIR, both employing a 50mm F2 lens).

Figure 6a shows the distribution of the dimensionless heat transfer coefficient (Nusselt number,  $Nu(x, y, t) = h(x, y, t) \cdot d / \lambda$ ) along two perpendicular symmetry lines - in the direction of the electrical current and across it, under this impinging jet. The figure shows that the jet is very symmetrical (at least for a combined width of 5 nozzle diameters) and that the measurement method is not strongly influenced by directional effects (such as reflection). Comparison of the values and their distribution to a well-established correlation from the literature [11] shows very good agreement, thereby supporting the optical properties previously found, and the described method.

In Fig. 6b, the transient response of the heater to flow start-up ("step function") is shown, wherein the valve located before the nozzle was suddenly opened. While the initial response of the heater is immediate it then follows a similar exponential convergence curve, regardless of the end-value flow rate. This type of curve is the characteristic response curve of an over-damped first order linear system, suggesting thermal dampening by the substrate (IR window).

### 3.1. Qualitative Transient measurement

Clearly, the instantaneous results measured from the transparent heater are not reliable. However, due to the rapid initial response, transient thermal phenomena can be qualitatively observed. Figure 7a shows an example of this through the case of a pulsating free-surface jet impingement on a vertical transparent heater. The jet has a nominal flow rate of  $Re=3300$  with pulsations in amplitude of about 10% at a frequency of 4.9Hz. The visual image, taken by high speed photography "through" the heater, shows the location of hydraulic jump (dashed line). Similarly, the thermal image shows a rapid increase in temperature around the same location. The temperature measured along a cross-sectional line is shown in figure 7b, at given time points within one cycle, reveal that the strongest temperature variations occur at a distance of 3 nozzle diameters from the stagnation point. This location coincides with the visually observed location of the hydraulic jump, suggesting that pulsating flow causes a periodic motion of the hydraulic jump, with a corresponding thermal oscillation measured at the wall.

## 4. Conclusions

In this experimental study the feasibility of IR thermography from a transparent heater, realized as a transparent conductive oxide coating on an IR window, has been demonstrated. In order to improve IR thermography from these partially transparent multi-layered heaters, optical properties were first accurately established. An experimental, highly IR-transparent coating was examined (CdO on a ZnS window), but was found to be too sensitive and damaged easily. Alternately, the ITO coatings had much lower transparency, but are more robust and commercially available. The transparency generally decreased with an increase in coating thickness, while the annealed type of ITO was found to have significantly higher emissivity, at the expense of its transparency. The apparent emissivity of all coatings was found to exponentially decay towards the actual value, with an increase in the temperature elevation (above the environment). Based on this observation, successful prediction of the emissivity can be obtained from measurements at relatively low temperature elevations, as may often be the limitation in cases of temperature sensitive liquids, proximity to phase-transfer or a limited calibration range.

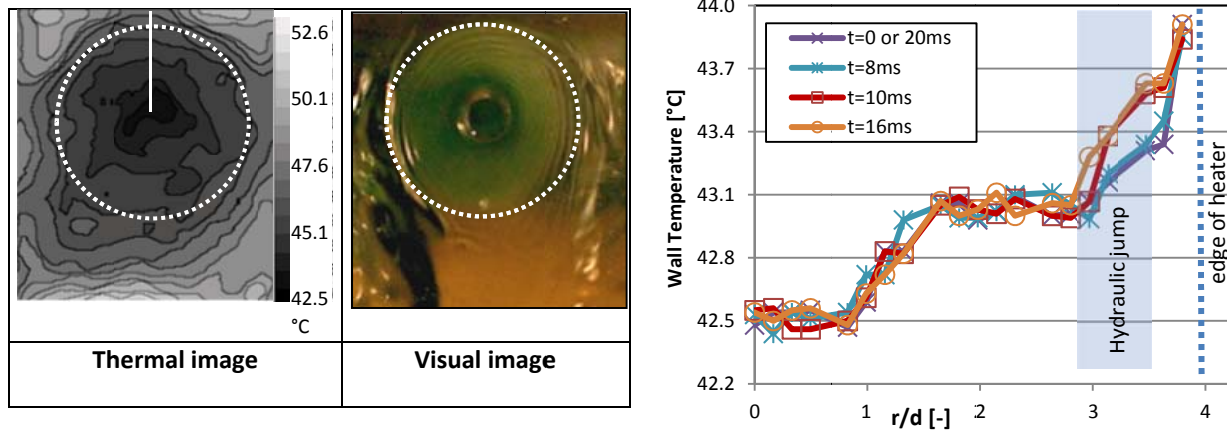


**Figure 7.** Free-surface jet impingement, oscillating flow: a) Thermal (wall) distribution and corresponding visual image ( $Re=3300$ ,  $q''= 3.7 \text{ W/cm}^2$ ), dashed line - location of hydraulic jump, white line - cross-section shown in b); b) Temperature distribution at several time points within one cycle, indicating the visually observed range of hydraulic jump position and the edge of the heater.

For the ITO coating examined in the steady submerged jet impingement test-case (100hm/sq. with no heat treatment), results were found to be consistent above a minimum temperature difference of  $0.5^\circ\text{C}$ , and good agreement with literature was shown, thereby substantiating the method. Although, the *transient* response of this transparent heater was found to be immediate (no time-delay observed) it was significantly dampened by the thermal response of the underlying IR window, rendering *quantitative* transient measurements impossible. However, *qualitative* thermal measurements are shown, for pulsating free-surface jet impingement, that clearly demonstrate its usefulness - the periodic motion of the hydraulic jump in this case was observed both visually and thermally.

Finally, it is recommended that when ITO is used, as in the present configuration, its emissivity should be experimentally established as shown. Generally, thinner/ higher resistivity annealed ITO has a higher combined transparency and emissivity, and should give a better signal without compromising its strength. These properties are crucial for IR thermography and may vary strongly between samples.

This study was conducted with funding by DFG project KN 764/3-1. We would also like to thank FLIR Systems, Germany, for loaning us the MWIR camera on short notice.

## References

- [1] Astarita T, Cardone G, Carlomagno G M and Meola C 2000 *Optics & Laser Tech.* **32** 593
- [2] Al-Sibai F, Leefken A, and Renz U 2002 *Int. J. Thermal Science* **41** 658.
- [3] Zimmermann A, Holland A M and Garner C P 2003 *Meas. Sci. Tech.* **14** 1648
- [4] Bang I C, Buongiorno J, Hu L W and Wang H 2008 *J. Power Energy Systems* **2** 340
- [5] Soriano G E, Alvarado J L and Lin Y P 2010 *Proc. Int. Heat Trans. Conf. (Washington D.C.)*
- [6] Soriano G E 2011 *Study of the Physics of Droplet Impement Cooling* Ph.D. Thesis, Texas A&M
- [7] Elison E, Webb 1994 *Int. J Heat Mass Trans.* **37** 1207
- [8] Webb B W and Ma C F 1995 *Adv. Heat Trans.* **26** 105
- [9] Bass M, Van Stryland E W, Williams D R, Wolfe W L 1995 *Handbook of Optics* (New York: McGraw Hill)
- [10] Haustein H D, Tebrügge G, Rohlf s W and Kneer R, Local heat transfer coefficient measurement through a visibly-transparent heater under jet-impingement cooling, *Int. J. Heat Mass Transfer* (2012), preprint: <http://dx.doi.org/10.1016/j.ijheatmasstransfer.2012.06.029>
- [11] Sun H, Ma and Tian Y Q 1997 *J. Thermal Science*, **6** (4) 286